J. Braz. Chem. Soc., Vol. 8, No. 2, 153-157, 1997.
Printed in Brazil.

0103 – 5053 $6.00 + 0.00

Article

An Electrochemical Impedance Spectroscopy Study of the Cobalt Electrodissolution Process in Carbonate-Bicarbonate Buffers

S.G. Real

Instituto de Investigaciones Fisicoquímicas Teóricas y Aplicadas (INIFTA), Facultad de Ciencias Exactas, Universidad Nacional de La Plata, Sucursal 4 - C.C. 16, (1900) La Plata, Argentina

Received: June 30, 1996; January 20, 1997

O processo de eletrodissolução do cobalto policristalino em soluções tamponadas de carbonato-bicarbonato, cobrindo faixas relativamente largas de força iônica, pH, e condições hidrodinâmicas da solução eletrolítica, têm sido investigado usando espectroscopia de impedância eletroquímica (EIS).

Os espectros de impedância foram analisados para determinar o comportamento dinâmico do sistema através da análise da função de transferência usando rotinas de ajuste não-linear e seguindo um modelo que fornece informações sobre os parâmetros característicos do processo eletroquímico na interface de reação. A análise dos dados das rotinas de ajuste não-linear mostraram que os espectros de impedância do processo de eletrodissolução do cobalto em tampões carbonato-bicarbonato para valores do pH entre 8.9 e 10.5 podem ser modelados considerando uma impedância de Warburg de comprimento finito que leva em consideração o processo de transporte de massa que ocorre no eletrólito.

The electrodissolution process of polycrystalline cobalt in carbonate-bicarbonate buffers covering relatively wide ranges of ionic strength, pH, and the hydrodynamic condition of the electrolyte solution, was investigated using electrochemical impedance spectroscopy (EIS).

Impedance spectra were analyzed to determine the dynamic behavior of the system by the application of transfer function analysis using non-linear fitting routines according to a model which gives information about the characteristic parameters of the electrochemical process at the reaction interface. Data analysis using non-linear fitting routines showed that the impedance spectra of the cobalt electrodissolution process in carbonate-bicarbonate buffers at pH 8.9-10.5 can be modeled considering a finite-length Warburg impedance that accounts for the mass transport process taking place in the electrolyte.

Keywords: *finite-length Warburg impedance, cobalt dissolution, carbonate-bicarbonate solutions*

Introduction

It is well known that bicarbonate ions and hydrodynamics have a considerable influence on the dissolution and passivation processes of polycrystalline iron[1], nickel[2], copper[3], and cobalt[4-6] electrodes in aqueous electrolytes. In particular, Co electrodes in solutions containing bicarbonate - carbonate ions exhibit higher electrodissolution current densities than in borate electrolytes at comparable anodic overpotentials[4]. From rotating disk electrode studies[6], it was concluded that the cobalt electrodissolution process in the prepassive potential range takes place through the formation of soluble Co(II) species, with the bicarbonate ions playing a fundamental role in the generation of a carbonate complex of Co(II).

The present paper aims to gain deeper insight into the mechanism of the Co electrodissolution process in carbonate-bicarbonate buffers covering a relatively wide range of ionic strength, pH, and hydrodynamics of the electrolyte

solution, using electrochemical impedance spectroscopy (EIS).

Experimental

The experimental setup was the same as that described in previous publications[7,8] . "Specpure" cobalt rotating disks (Johnson Matthey Chemicals, 0.070 cm^2 apparent area), axially embedded in PTFE holders, were used as working electrodes. Prior to each electrochemical experiment, the working electrodes were mechanically polished with 400 and 600 grade emery papers, and with 1.0 and 0.3 μm grit alumina-acetone suspensions, thoroughly rinsed in triply distilled water, and cathodically polarized for 1 min in the hydrogen evolution reaction potential range. Potentials were measured against a SCE, making contact with the solution through a Luggin-Haber capillary tip properly shielded to avoid chloride ion diffusion. Potentials in the text are referred to the NHE scale.

The electrolyte solutions consisted of a mixture of x M $KHCO_3$ + y M K_2CO_3 ($0.075 \leq x \leq 2.25$; $0.05 \leq y \leq 1.5$), $8.9 \leq pH \leq 10.5$. They were prepared from analytical grade (p.a. Merck) reagents and triply distilled water. Experiments were carried out under purified N_2 gas saturation at 25 °C. The working electrode was maintained either at rest or under rotation at speed w (300 rpm ≤ w ≤ 2500 rpm).

Impedance measurements were carried out using a Solartron 1250 FRA and 1186 EI integrated with a PC system. Detailed descriptions of both the hardware arrangement and the data processing, including non-linear fitting routines and parametric identification procedures, have been given elsewhere[7-9].

Results and Discussion

Figures 1 and 2 show the Nyquist diagrams for the active Co dissolution at w = 1000 rpm in various electrolyte solutions, at the potentials marked in the corresponding steady-state polarization curves (j *vs.* E). The general features of the frequency response of the Co electrodissolution reaction in different carbonate-bicarbonate buffers do not differ significantly. The complex plane plots display two slightly distorted capacitive semicircles in the 50 kHz ≥ f ≥ 2 mHz frequency range, with $f = \omega/2\pi$. It is worth noting that the frequency corresponding to the maximum of the capacitive loop at the lower frequencies is about 0.5 Hz, this value being practically independent of both solution composition and operational potential in nearly the entire active metal dissolution potential range, although it diminishes to about 0.3 Hz at potentials close to the corresponding open circuit corrosion potential, E_{corr}. At each operational potential the experimental impedance extrapolated at $\omega \rightarrow 0$ yielded a value of the polarization resistance $R_p = \lim_{\omega \rightarrow 0} |Z(j\omega)|$ in good agreement with that corresponding to the slope of the stationary polarization curve expressed as $R_p = (\partial E/\partial j)$.

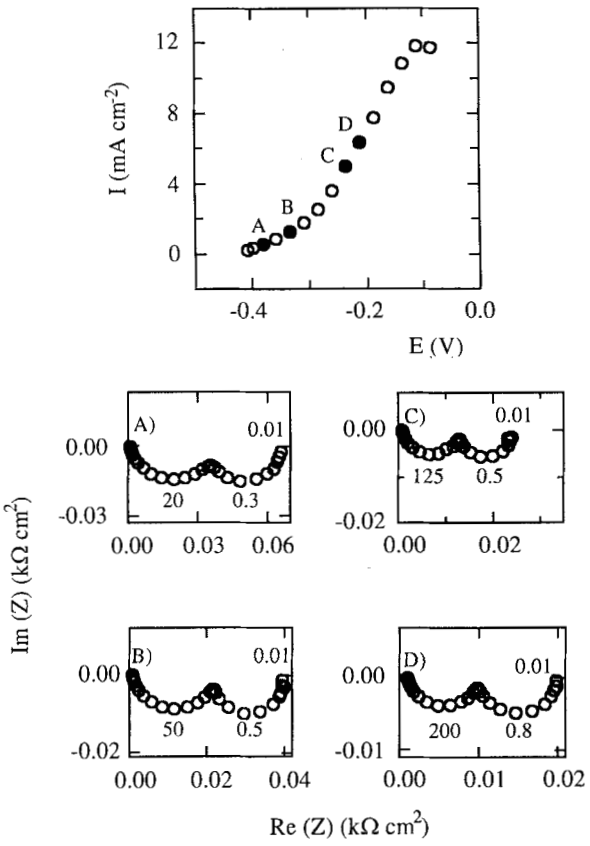

Figure 1. Impedance diagrams at the polarization points marked on the steady-state polarization curve (j *vs.* E) for Co in 2.25 M $KHCO_3$ + 0.15 M K_2CO_3, pH = 8.9, w = 1000 rpm. A) E = -0.380 V; B) E = -0.310 V; C) E = -0.260 V; D) E = -0.235 V.

The effect of w on impedance diagrams can be evaluated from Figs. 3a and 3b, measured at low and intermediate anodic polarizations, respectively. At a constant potential and increasing w, the chord related to the high frequency loop becomes smaller, the frequency at the maximum of the capacitive contribution at lower frequencies increases and the polarization resistance, R_p, diminishes remarkably.

A fairly good description of the impedance diagrams was obtained using non-linear fitting routines according to the following total transfer function $Z_T(j\omega)$:

$$Z_T(j\omega) = R_\Omega + Z(j\omega) \quad (1)$$

where R_Ω is the electrolyte resistance contribution and $Z(j\omega)$ is given by:

$$[Z(j\omega)]^{-1} = [CPE]^{-1} + [Z_f(j\omega)]^{-1} \quad (2)$$

with the faradaic impedance $Z_f(j\omega)$ expressed as

$$Z_f(j\omega) = R_t + R_{DO}(jS)^{-1/2} \tanh(jS)^{1/2} \quad (3)$$

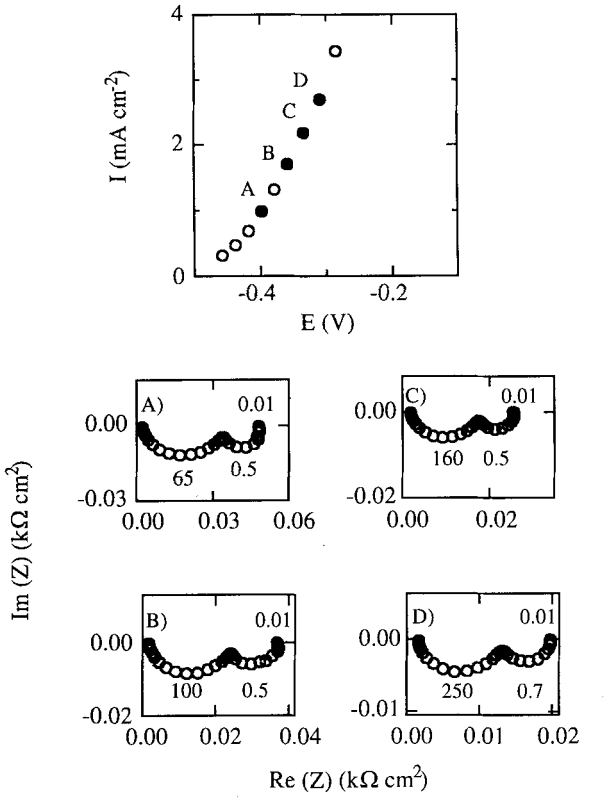

Figure 2. Impedance diagrams at the polarization points marked on the steady-state polarization curve (j *vs.* E) for Co in 0.75 M $KHCO_3$ + 1.5 M K_2CO_3, pH = 10.5, w = 1000 rpm. A) E = -0.380 V; B) E = -0.360 V; C) E = -0.335 V; D) E = -0.310 V.

In Eq. 2 the constant phase element, $CPE = [C_{dl}(j\omega)^{\alpha}]^{-1}$, involves the double layer capacitance, C_{dl}, and the parameter α that takes into account the distribution of time constants due to surface inhomogeneities, whereas in Eq. 3 $Z_f(j\omega)$ includes the contribution of the charge transfer resistance, R_t, defined as the $\omega \rightarrow \infty$ limit of $Z_f(j\omega)$, and a finite diffusion impedance, Z_W, defined as:

$$Z_W = R_{DO}\,(jS)^{-1/2}\tanh(jS)^{1/2} \qquad (4)$$

The latter was considered in order to account for the mass transport process involved in the Co electrodissolution reaction. The diffusion resistance, R_{DO}, is the $\omega \rightarrow 0$ limit of a finite-length Warburg impedance, $S = \delta^2\omega/D$, δ and D being the diffusion length and the diffusion coefficient, respectively. Accordingly, R_p corresponds to the $\omega \rightarrow 0$ limit of the $Z_T(j\omega)$, defined according to Eqs. 1 to 3. Furthermore, the time constant $\tau_D = 2\delta^2/D$ associated with finite diffusion impedance[10,11] can be related to the inverse of the frequency value at which the diffusion impedance attains the maximum on the imaginary axis and can be expressed as $\tau_D = 2S(\omega_{max})^{-1}$. Consequently, it becomes clear that τ_D is independent of the polarization potential, although it depends on both δ and D. On the other hand,

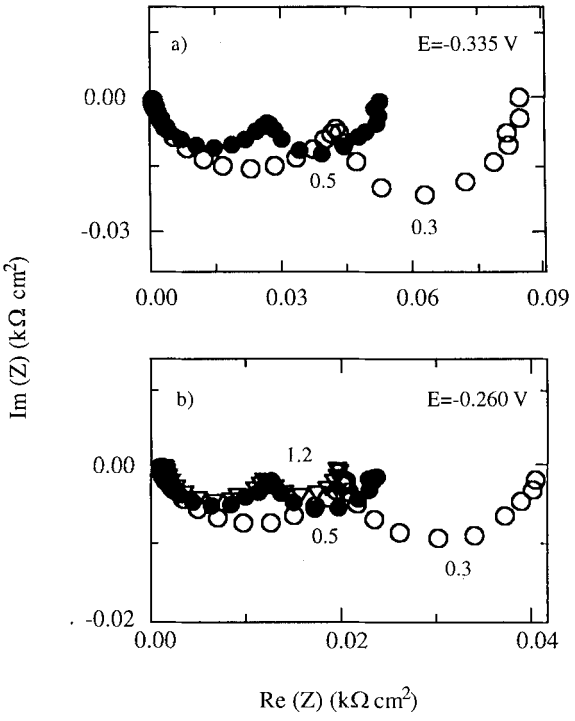

Figure 3. Influence of w on impedance diagrams for Co in 2.25 M $KHCO_3$ + 0.15 M K_2CO_3, pH = 8.9, a) E = -0.335 V,(0) w = 300 rpm, (0) w = 1000 rpm; b) E = -0.260 V, (0) w = 300 rpm, (0) w = 1000 rpm, (▽) w = 2500 rpm.

taking into account the influence of hydrodynamics on kinetic results, δ can be related to the thickness of the diffusion layer which decreases with increasing w. The good agreement between the experimental and calculated data according to the transfer function model given in Eqs. 1-4 is shown in Figs. 4 to 6.

From the optimum fit of the CPE parameter derived from the high frequency loop in the whole set of experiments, values of α close to 0.9 and of the double layer capacitance of about 25-65 $\mu F\ cm^{-2}$ were obtained. Tables 1 to 3 show the transfer function parameters obtained from the fitting procedure at different polarization conditions in a 2.25 M $KHCO_3$ + 0.15 M K_2CO_3 solution at pH = 8.9, and w = 1000 rpm (Table 1); in a 0.75 M $KHCO_3$ + 1.5 M K_2CO_3 solution at pH = 10.5, and w = 1000 rpm (Table 2); and at different hydrodynamic conditions (Tables 3.a and 3.b).

At each w, the value of δ was calculated according to the rotating disk electrode theory[12] by the expression:

$$\delta = 1.61\,(D/\nu)^{1/3}\,(\nu/w)^{1/2} \qquad (5)$$

and assuming that in aqueous solutions the Schmidt number, $Sc = \nu/D$, yields approximately equal to 10^3 [12], where ν is the kinematic viscosity of the solution. Therefore, taking into account that δ^2/D is a fitting parameter from the values of D estimated at various potentials for all the

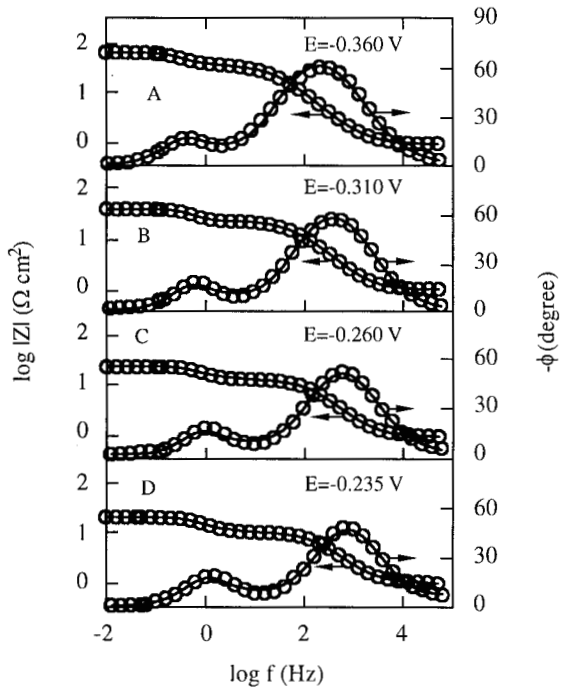

Figure 4. Comparison of the experimental (o) and simulated (---) Bode plots at the polarization points marked in Fig. 1 for Co in 2.25 M $KHCO_3$ + 0.15 M K_2CO_3, pH = 8.9, w = 1000 rpm.

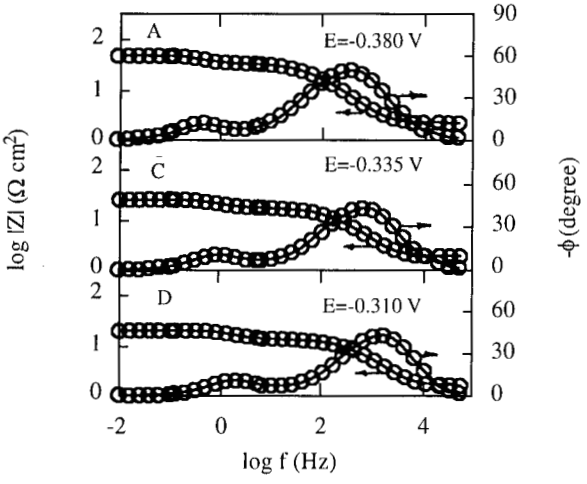

Figure 5. Comparison of the experimental (o) and simulated (---) Bode plots at the polarization points A, C and D, marked in Fig. 2 for Co in 0.75 M $KHCO_3$ + 1.5 M K_2CO_3, pH = 10.5, w = 1000 rpm.

studied electrolyte compositions, it is possible to derive a mean value of $D \cong (3.0 \pm 0.5) \times 10^{-6}$ cm^2 s^{-1} which agrees well with the expected values for an ion diffusion process in aqueous solutions[13].

The presence of the slight frequency distribution observed in the high frequency loop is not enough evidence of the presence of two distinct time constants. However, if the first step is fast and reversible or the pseudocapacitance value is on the same order of magnitude as the double layer

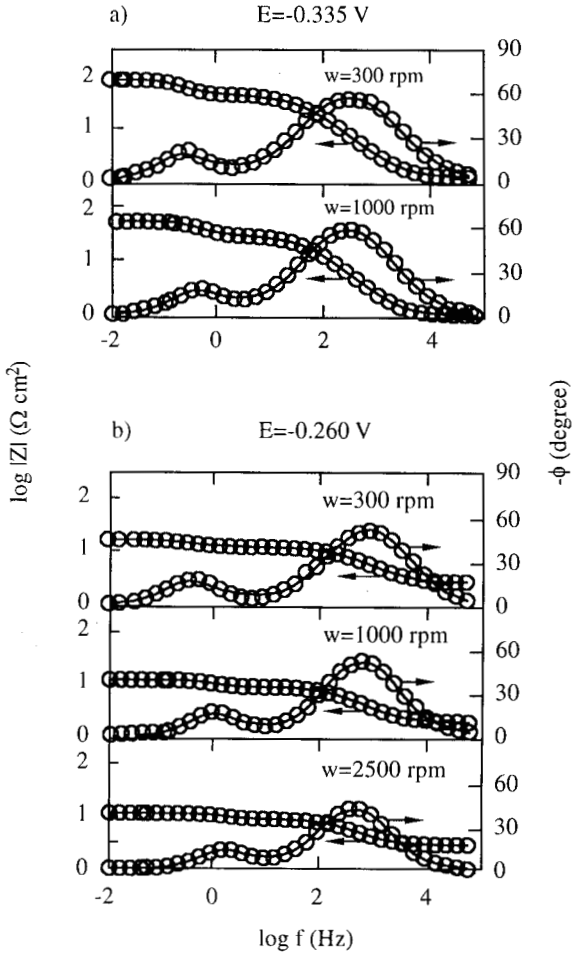

Figure 6. Comparison of the experimental (o) and simulated (---) Bode plots at the polarization points marked in Fig. 3 for Co in 2.25 M $KHCO_3$ + 0.15 M K_2CO_3, pH = 8.9, under different hydrodynamic conditions: a) E = -0.335 V, w = 300 and 1000 rpm; b) E = -0.260 V, w = 300, 1000 and 2500 rpm.

capacitance, the time constant cannot be observed experimentally. According to this analysis, and taking into account that the two electron transfer reaction is less likely to occur, the reaction steps considered in a model with a minimal degree of complexity have to involve at least one Co(I) intermediate species. It has been reported[4,6] that the solubility of Co(II) in $KHCO_3$ solutions of varying concentration at pH 8.4 is proportional to the concentration of HCO_3^- in solution until the solubility product of $CoCO_3$ is reached. However, in the presence of excess HCO_3^- ions, $CoCO_3$ redissolves as the complex ion $Co(CO_3)_2^{2-}$. The existence of this complex ion has been confirmed by visible absorption spectroscopy[4]. Consequently, and considering the present results, the Co electrodissolution process in carbonate-bicarbonate buffers of pH 8.9-10.5 should be interpreted in terms of a model that involves mass transfer control, where diffusion of either HCO_3^- species to the

Table 1. Values of the transfer function parameters obtained from the fitting procedure at the polarization points marked in Fig. 1. for Co in 2.25 M $KHCO_3$ + 0.15 M K_2CO_3, pH = 8.9, w = 1000 rpm.

E V	R_Ω Ω cm^2	C_{dl} μFcm^{-2}	R_t Ω cm^2	$\delta/D^{1/2}$ s$^{1/2}$	R_{DO} Ω cm^2
-0.380	0.98	65	47.67	1.02	28.00
-0.310	0.91	64	19.11	1.04	20.86
-0.260	0.91	65	10.99	0.90	12.81
-0.235	091	55	8.12	0.82	10.78

Table 2. Values of the transfer function parameters obtained from the fitting procedure at the polarization points marked in Fig. 2. for Co in 0.75 M $KHCO_3$ + 1.5 M K_2CO_3 pH = 10.5, w = 1000 rpm.

E V	R_Ω Ω cm^2	C_{dl} μFcm^{-2}	R_t Ω cm^2	$\delta/D^{1/2}$ s$^{1/2}$	R_{DO} Ω cm^2
-0.380	1.53	27	29.75	1.04	17.29
-0.360	1.54	28	21.00	0.92	13.09
-0.335	1.82	26	15.12	0.91	9.03
-0.310	1.54	29	11.06	0.80	7.49

Table 3a. Values of the transfer function parameters obtained from the fitting procedure for Co in 2.25 M $KHCO_3$ + 0.15 M K_2CO_3 at E = -0.335 V under the different hydrodynamic conditions shown in Fig. 3a.

w rpm	R_Ω Ω cm^2	C_{dl} μFcm^{-2}	R_t Ω cm^2	$\delta/D^{1/2}$ s$^{1/2}$	R_{DO} Ω cm^2
300	1.19	28	37.94	1.50	53.8
1000	0.91	65	24.36	1.00	28.0

Table 3b. Values of the transfer function parameters obtained from the fitting procedure for Co in 2.25 M $KHCO_3$ + 0.15 M K_2CO_3 at E = -0.260 V under the different hydrodynamic conditions shown in Fig. 3b.

w rpm	R_Ω Ω cm^2	C_{dl} μFcm^{-2}	R_t Ω cm^2	$\delta/D^{1/2}$ s$^{1/2}$	R_{DO} Ω cm^2
300	1.19	25	18.90	1.40	22.33
1000	0.91	65	10.99	0.90	12.81
2500	1.54	53	10.15	0.60	8.40

electrode surface or $Co(CO_3)_2^{2-}$ from the surface is likely to occur.

Conclusions

An electrochemical impedance study of cobalt in carbonate-bicarbonate solutions has been reported. In general, the impedance spectra display two slightly distorted capacitive relaxations in the 50 kHz-2 mHz frequency range. According to the characteristics of the frequency at the maximum of the slightly distorted capacitive loop at low frequencies, the impedance response was modeled considering a finite-length Warburg impedance that accounts for the mass transport process taking place in the electrolyte. The analysis also suggests that changes in the diffusion layer thickness can be monitored *in situ* by impedance measurements. It is proposed that the dissolution reaction of Co in carbonate-bicarbonate buffers of pH 8.9-10.5 involves a mass transfer control, where the diffusion of either HCO_3^- species to the electrode surface or $Co(CO_3)_2^{2-}$ species from the surface is likely to occur.

Acknowledgments

This research project was financially supported by the Consejo Nacional de Investigaciones Científicas y Técnicas (CONICET) of Argentina. The author wishes to thank Prof. J.R. Vilche for useful discussions.

References

1. Castro, E.B.; Vilche, J.R. *J. Electroanal. Chem.* **1992**, *323*, 23.
2. Boh A.E.; Vilche, J.R.; Arvia, A.J. *J. Appl. Electrochem.* 1990, *20*, 418.
3. Ribotta, S.B.; Folquer, M.F.; Vilche, J.R. *Corrosion* **1995**, *51*, 682.
4. Davies, D.H.; Burstein, G.T. *Corros. Sci.* **1980**, *20*, 973.
5. Burstein, G.T.; Davis, D.H. *Corros. Sci.* **1980**, *20*, 989().
6. Gervasi, C.A.; Biaggio, S.R.; Vilche, J.R.; Arvia, A.J. *Corros. Sci.* **1989**, *27*, 427.
7. Real, S.G.; Vilche, J.R.; Arvia, A.J. *J. Electroanal. Chem.* **1992**, *341*, 181.
8. Castro, E.B.; Real, S.G.; Milocco, R.H.; Vilche, J.R. *Electrochim. Acta* **1991**, *36*, 117.
9. Castro, E.B.; Real, S.G.; Saidman, S.B.; Vilche J.R.; Milocco, R.H. *Materials Science Forum* **1989**, *44/45*, 417.
10. Buck, R.P. *J. Electroanal. Chem.* **1977**, *18*, 363.
11. Dawson, J.; Jhon, D. *J. Electroanal. Chem.* **1980**, *110*, 37.
12. Pleskov, Yu. V.; Filinovskii, Yu In *The Rotating Disc Electrode*; New York, 1976.
13. Bruins, H.R. In *International Critical Tables of Numerical Data, Physics, Chemistry and Technology;* Washburn, E.W., Ed.; McGraw-Hill; N.Y., Vol.V, 1929, p. 69.